Reports

Physical Conditions at the Base of a Fast Moving Antarctic Ice Stream

HERMANN ENGELHARDT, NEIL HUMPHREY, BARCLAY KAMB, MARK FAHNESTOCK

Boreholes drilled to the bottom of ice stream B in the West Antarctic Ice Sheet reveal that the base of the ice stream is at the melting point and the basal water pressure is within about 1.6 bars of the ice overburden pressure. These conditions allow the rapid ice streaming motion to occur by basal sliding or by shear deformation of unconsolidated sediments that underlie the ice in a layer at least 2 meters thick. The mechanics of ice streaming plays a role in the response of the ice sheet to climatic change.

THE DEMONSTRATION OF RAPID MOTIONS in the great Antarctic ice streams (*1*) has added an important new element to earlier concern over the possible instability of the West Antarctic Ice Sheet (*2*), because these motions provide a process for rapid dispersal and disintegration of the ice sheet. This process needs to be taken into consideration in attempting to evaluate the interactive role of the ice sheet in global change. To do this in a reliable way requires an understanding of the underlying physical mechanism of ice streaming flow. Concentrated glaciological study of the Siple Coast sector of the ice sheet in recent years has delivered good data on ice stream morphology, motions, and mass balance (*1, 3, 4*), which provide basic information relevant to the physical mechanism of ice streaming. To the earlier suggested mechanisms of ice superplasticity (*5*) and basal sliding (*6*) has been added a new hypothesis based on detailed seismic sounding, namely, that the rapid motions are due to shear deformation of a layer of water-saturated till underlying the ice (*7*).

Quantitative models of ice stream flow have been developed (*8, 9*), but until the actual streaming flow mechanism is known, these theoretical models can only be considered to be hypothetical. Observations are therefore needed to distinguish as directly as possible among the different proposed mechanisms for rapid flow.

In this report, we present initial results of a program of drilling to the base of ice stream B to determine physical conditions there and to relate them to the rapid motion. The work was carried out in November 1988 to January 1989 and in December 1989. It complements borehole geophysical observations (*10*) at Crary Ice Rise, some 150 km beyond where ice stream B goes afloat and is incorporated into the Ross Ice Shelf.

The West Antarctic ice streams are rapidly moving currents 30 to 80 km wide and 300 to 500 km long within the generally slow-moving mass of the ice sheet [Fig. 1 (*4*)]. Flow velocities in ice stream B are 0.3 to 2.3 m per day, compared to about 0.02 m per day in the adjacent ice sheet (*1*). The rather sharp boundaries between ice stream and adjacent ice sheet are shear zones about 5 km wide that are marked at the surface by a prominent band of chaotic crevassing.

Our work on ice stream B was carried out at field camp Upstream B (83.5°S, 138.2°W) (Fig. 1), where the flow velocity is 1.2 m per day (*1*). With the hot water drilling method (*11*), we drilled five boreholes to the bottom of the ice stream in 1988 and three in 1989. The holes were drilled within an area about 200 m by 500 m. The bottom was encountered at depths of 1030 to 1037 m in 1988 and 1057 to 1058 m in 1989, in approximate agreement with the depth of 1070 m indicated at Upstream B in the ice thickness map of Shabtaie and Bentley (*3*), which was based on radio echo sounding. The ambient near-surface ice temperature of about −25°C caused rapid refreezing of the water-filled boreholes, which posed a threat to the drilling operation and limited the use of the holes for instrumental observations to a period of only ~6 hours after the last reaming to 10-cm diameter. The holes were used to measure a temperature profile, to record basal water pressure, and to carry out penetrometry and sampling of the subglacial material.

The temperature values plotted in Fig. 2 were obtained by two different data reduction procedures. The open circles were obtained by extrapolation of measured borehole temperature versus time curves to infinite time by the standard procedure (*12*). The temperature sensor system (*13*) suffered electrical malfunctions under high water pressure, which introduced a common mode noise component into the readings of all sensors and caused complete loss of data from depths within 110 m of the bottom. The crosses in Fig. 2 were obtained by a procedure to remove the common mode noise, plus introduction of in situ calibration from initial sensor readings in the ice water of the borehole before the hole froze in (*14*). The difference between the cross and circle values at each depth, and the scatter of the

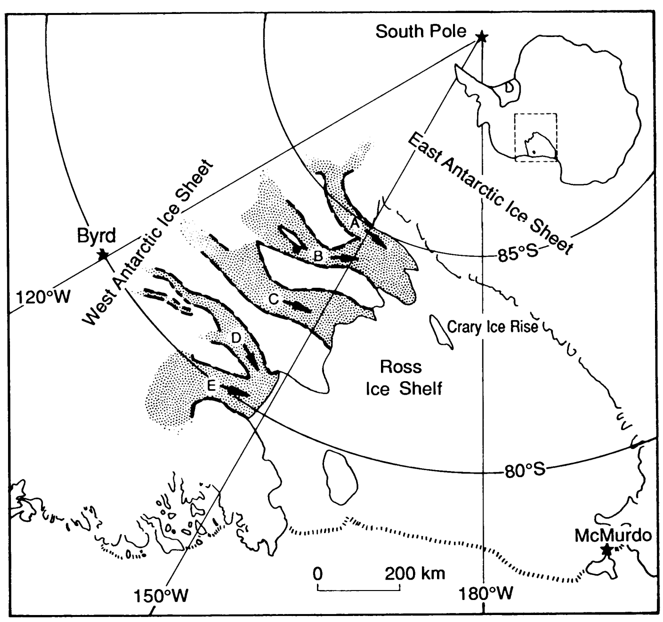

Fig. 1. Location map of ice streams in the West Antarctic Ice Sheet flowing into the Ross Ice Shelf (*4*). Ice streams (stippled) are labeled by their letter designations. Marginal shear zones are shown with heavy dashed lines. The grounding line at the inner edge of the Ross Ice Shelf is shown with a solid line, and the outer calving edge with a hachured line. Major Antarctic stations are marked with a star, and the field camp Upstream B is marked with a heavy dot at 83.5°S, 138°W. Inset at upper right shows map area in relation to the Antarctic continent.

Division of Geological and Planetary Sciences, California Institute of Technology, Pasadena, CA 91125.

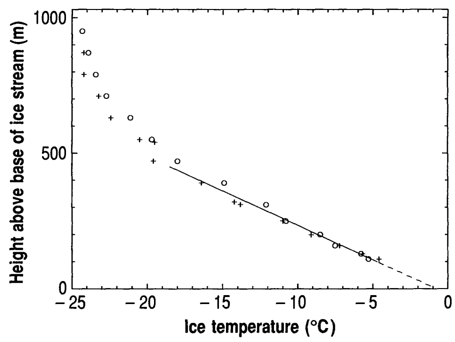

Fig. 2. Temperature profile through ice stream B at field station Upstream B. Open circles and crosses give temperature values obtained from measured temperatures by two different data-reduction procedures as described in the text. The straight line is a least-squares fit to the data points below 400 m and is extrapolated (dashed) to the bottom.

points from a smooth curve, give a measure of uncertainty in the temperature values, which is about ±1°C (*15*). Straight line extrapolation to the bottom of the hole (Fig. 2) indicates a basal temperature of −1 ± 1°C. This value is compatible with a basal temperature of −0.7°C, which is the melting temperature at the overburden pressure of 91 bars (*16*).

During drilling, borehole water levels stood at a depth of about 30 m, near the firn-ice transition (*17*). In all cases, when the drill reached the bed, as indicated by abrupt cessation of drill advance, the water level dropped to about 110 m below the surface. In seven of the holes the drop was immediate or within about 3 min of reaching the bed; in one hole (borehole 2) it occurred about 9 hours later. The drop in water level shows that the boreholes become connected to a basal water conduit system and thus that the ice is not frozen to the bed (*18*), which is compatible with the extrapolated temperature profile, as described above. The basal water system accepted on average about 2 m^3 of water in each water level drop event.

The observation of melting conditions at the base of ice stream B confirms a prediction by Rose (*6*) based on calculations of the temperature at depth. The heat, 0.2 W m^{-2}, generated in the basal zone by sliding at a speed of 1 m per day (or by the equivalent basal or sub-basal shear deformation), combined with the inflow of geothermal heat from below ($\gtrsim$0.04 W m^{-2}) (*17, 19*), substantially exceeds the upward heat flow of 0.08 W m^{-2} in the lower half of the ice stream (calculated for conduction in the temperature gradient shown in Fig. 2). The excess heat results in an equivalent amount of melting of basal ice if a thermal steady state prevails.

The depth to which the water level dropped on reaching the bed in the different holes in 1988 was 102 to 115 m (individual values were 102, 111, 105, 109, and 115 m), and in the 1989 holes it was 111 to 115 m. This level is close to the flotation level, that is, the water level at which the basal water pressure in communication with the borehole is equal to the ice overburden pressure at the bed. The depth of the flotation level depends on the ice density profile, which is known to a depth of 50 m from core data (*17*). If for the density profile at greater depth we use data (*19*) from the deep core at Byrd Station (Fig. 1), adjusted to the temperature profile at Upstream B (*20*), we find the flotation level to be at a depth of 99 m for an ice thickness of 1035 m, appropriate to the 1988 holes, and at a depth of 101 m for an ice thickness of 1057 m, appropriate to the 1989 holes. On this basis, the observed basal effective confining pressure (overburden pressure minus water pressure) in the different boreholes varied from 0.3 to 1.6 bars. This can be compared with the value 0.5 ± 0.4 bar inferred by Blankenship *et al.* (*7*) from seismic data.

Figure 3 shows the time variation of water pressure (expressed as equivalent borehole water level) measured with a pressure transducer at the bottom of borehole 3. The first pressure rise, 12 hours after the initial water level drop to 105 m, occurred at about the time when (according to theoretical calculations) one would expect the borehole to first freeze shut at a point in the upper part of the hole where the temperature is lowest (Fig. 2). Subsequent freezing below this point will tend to inject water from the borehole into the basal water system because of the expansion on freezing. Perhaps the first pressure rise was caused by this injection and reflected a detectable impedance in the local water system or in the borehole's connection to it. We do not yet have a clear idea as to the cause of the second rise and associated details (*21*).

Samples of rock material from the basal zone were obtained by three different methods. In the first, fine granular material driven into suspension by the hydraulic-mining action of the hot water drill jet was captured as it settled out in open chambers in the drill stem. In this way we obtained 2 kg of bottom sediment from borehole 2. The sample consists of fine sand and silt, similar to the fine sediment fractions obtained at the bed in other glaciers, except for the relative lack of the finest (clay size) fraction, which was mostly winnowed out in the sampling procedure. Under microscopic examination we found several sponge spicules; these indicate that the material contains marine sediment. A portion of the sample was examined by Scherer (*22, 23*), who reported the presence of marine and nonmarine diatom tests and several other microfossil types, both terrestrial and marine. The diatoms are of a mixture of Cenozoic ages including examples from the Ogliocene, Miocene, Pliocene, and possibly Pleistocene (*22*).

In the second sampling method a borehole penetrometer, consisting of a steel rod of 1.2-cm diameter with a sharpened tip, was driven into the bottom by a heavy cylindrical hammer weight. A layer of sediment about 2 mm thick with coarse particles protruding adhered to the rod up to 0.4 m above the tip and was recovered (total sample weight 12 g). Because this sediment was sampled in place, without the winnowing and size-sorting action involved in the first method, the second method yielded a more representative and less disturbed sample. The material is a muddy, unsorted mixture with clasts up to 7 mm in size. The coarse clasts are mostly granitic, some with gneissic structure. The particle size distribution of the sample (Fig. 4) falls near the middle of the range for Pleistocene deposits considered to be basal tills (*24*). This similarity suggests that at the sampling point, ice stream B has unconsolidated till at its base. An alternative possibility, that the material sampled came from frozen englacial till released from the ice by hot water drilling, can be ruled out because clay-size material, which would have been winnowed out by the jet drilling action (as in the first sample), is abundant. The hydraulic permeability of the second sample, measured in a small falling-head permeameter, was 2 × 10^{-9} m

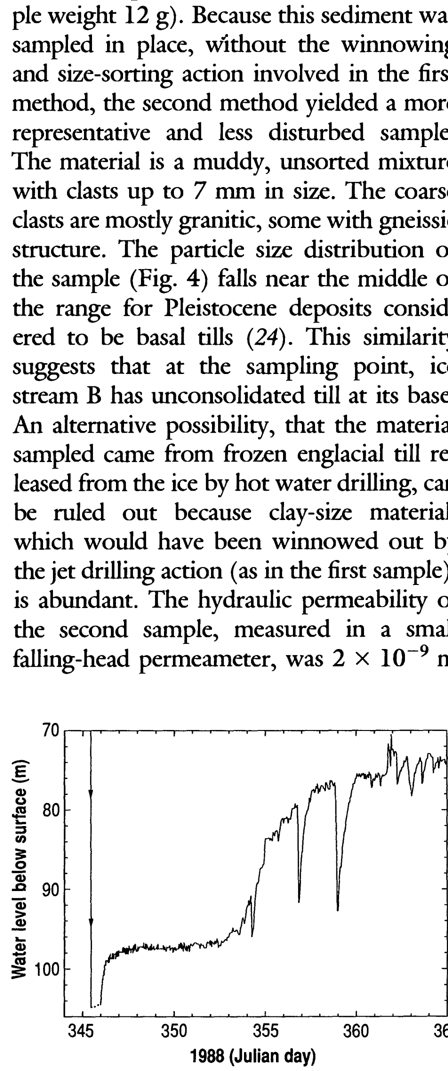

Fig. 3. Basal water pressure versus time in borehole 2 at Upstream B. Pressure is shown in terms of the equivalent depth of the borehole water level below the surface. The time scale is in Julian days (JD 345 is 11 December). The rapid initial drop in water level upon borehole completion is the near vertical line with arrowheads, at JD 345.5. The subsequent record was obtained with a pressure transducer placed at the bottom. There are no data over the interval JD 345.5 to 346.0.

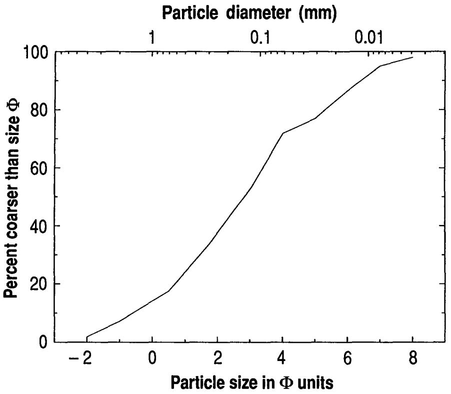

Fig. 4. Particle size distribution analysis of subglacial sediment from the base of ice stream B. The abscissa gives particle size d expressed in terms of the standard variable $\Phi = -\log_2 (d/d_0)$ where $d_0 = 1$ mm. A scale for d is at the top. The ordinate is the cumulative size distribution, that is, the percentage (by weight) of particles coarser than any given size.

s^{-1}. This value lies in the permeability range of 10^{-12} to 10^{-6} m s^{-1} observed for glacial tills (*25*).

The third sampling method was piston coring. In December 1989 we obtained two piston cores, each 2 m long and 5 cm in diameter, from beneath the ice near Upstream B. When the subglacial material was recovered, it was unfrozen, plastic, and clayey to the touch, but also gritty from coarser particles. The material contains rock clasts as large as 5 cm. It appears to lack bedding or other structural layering. These attributes reinforce the conclusion that the subglacial material is till and that the base of the ice is at the melting point. Measurement of weight loss on drying indicates that the water-saturated porosity is 40 ± 1% (two samples); this high porosity suggests that the till has been dilated by active shear deformation.

The basal sampling provides direct observations of a subsole till layer of the general type inferred from seismic data (7). The length of the cores indicates that the layer is at least 2 m thick. The seismically inferred thickness is about 6.5 m in the vicinity of Upstream B (*26*). Indications that the till has been deformed are its high porosity and the mixture of ages of its contained fossils, which suggests that mixing of rock materials from a variety of bedrock sources has occurred, as could be expected in a deforming subsole till (*22*).

The observations that ice stream B is melting at its base and that the basal water pressure is near the ice overburden pressure have strong implications for the mechanics of ice stream flow. The melting condition allows mechanisms of basal sliding and subbasal sediment deformation to operate. High basal water pressures, near flotation, promote rapid basal sliding, as has been observed in glacier surging (*27*) and laboratory experiments (*28*) and as expected from theoretical considerations (*29*). High water pressure also reduces strength and promotes deformability of unconsolidated, water-saturated sediments (*30*). The presence of a layer of deformable sub-basal till, inferred from seismic data (7), is confirmed by our borehole sampling. The proportions of the ice stream motion due to basal sliding, subglacial till deformation, and ice superplasticity remain unknown, however.

REFERENCES AND NOTES

1. I. M. Whillans, J. Bolzan, S. Shabtaie, *J. Geophys. Res.* **92**, 8895 (1987).
2. T. J. Hughes, *ibid.* **78**, 7884 (1973); J. Weertman, *ibid.* 66, 3783 (1961).
3. S. Shabtaie and C. R. Bentley, *Ann. Glaciol.* **11**, 126 (1988).
4. S. Shabtaie, I. M. Whillans, C. R. Bentley, *J. Geophys. Res.* **92**, 8865 (1987); C. R. Bentley, *ibid.*, p. 8843; S. Shabtaie and C. R. Bentley, *ibid.*, p. 1311; I. M. Whillans and R. A. Bindschadler, *Ann. Glaciol.* **11**, 187 (1988); S. Shabtaie, C. R. Bentley, R. A. Bindschadler, D. R. MacAyeal, *ibid.*, p. 137.
5. T. J. Hughes, *Rev. Geophys. Space Phys.* **15**, 1 (1977).
6. K. E. Rose, *J. Glaciol.* **24**, 63 (1979).
7. D. D. Blankenship *et al.*, *Nature* **322**, 54 (1986); R. B. Alley, D. D. Blankenship, S. T. Rooney, C. R. Bentley, *ibid.*, p. 57; D. D. Blankenship, C. R. Bentley, S. T. Rooney, R. B. Alley, *J. Geophys. Res.* **92**, 8903 (1987); R. B. Alley, D. D. Blankenship, C. R. Bentley, S. T. Rooney, *ibid.*, p. 8921.
8. R. A. Bindschadler, *J. Glaciol.* **29**, 3 (1983); C. S. Lingle and T. J. Brown, in *The Dynamics of the West Antarctic Ice Sheet*, C. J. van der Veen and J. Oerlemans, Eds. (Reidel, Dordrecht, 1987), pp. 249–285; J. Weertman and G. E. Birchfield, *Ann. Glaciol.* **3**, 316 (1982).
9. R. B. Alley *et al.*, *J. Geophys. Res.* **92**, 8931 (1987); *J. Glaciol.* **35**, 130 (1989).
10. R. Bindschadler *et al.*, *Ann. Glaciol.* **12**, 199 (1989).
11. P. L. Taylor, in *Ice Drilling Technology*, G. Holdsworth, K. C. Kulvinen, J. H. Rand, Eds. (*Spec. Rep. 84-34*, U.S. Army Cold Regions Research Engineering Laboratory, Hanover, NH, 1984), pp. 105–117; H. Engelhardt and J. Determann, *Nature* **327**, 380 (1987).
12. The temperature data values at a given depth are plotted against reciprocal time since the borehole froze in at that depth; the temperature is extrapolated to infinite time by a straight line fit to the data in this plot; A. H. Lachenbruch and M. C. Brewer, *U.S. Geol. Surv. Bull. 1083-C* (1959), p. 77.
13. The temperature sensors were AD 590 monolithic integrated circuit temperature transducers, operated in a current sinking mode, and cast in epoxy to resist entry of water. The sensors could be read to ±0.1°C (SE), and were calibrated at 0°C before use. Signals from 32 sensors were multiplexed onto an eight-conductor cable with the help of an MC4067 analog multiplexer paired with each sensor.
14. Common mode noise caused by the electrical malfunctions was filtered from the temperature versus time records as follows: For a reference sensor at depth 80 m, which was 20 m above the water level, the data in a temperature versus reciprocal time plot were fit to a straight line, and straight line values were then subtracted from the data to give effectively a high-pass filtered noise curve. This noise curve was subtracted from the data plots for the other sensors to remove the common mode noise. This resulted in considerable smoothing of the data plots and allowed more reliable extrapolation to infinite time. Use of in situ calibration avoids drift in sensor output from the time of calibration to the time of use down hole, and it allows an effect of water pressure on sensor output to be included in the calibration.
15. SD values calculated from the data in Fig. 2 are 0.6°C for both measures of uncertainty (difference between cross and circle values; scatter of points about a smooth curve).
16. The effect of solutes on the melting point is probably small and is disregarded.
17. R. B. Alley and C. R. Bentley, *Ann. Glaciol.* **11**, 1 (1988).
18. This interpretation of the water-level drop might appear contradicted by the observation of a loss of 50 liters of water from the bottom of a borehole in the Agassiz Ice Cap, Ellesmere Island, and of about 4.4 m^3 of diesel oil from another borehole in the same ice cap, where the basal temperature was about −19°C and the ice was inferred to overlie a porous substrate that had been ice-free during the last interglacial [R. M. Koerner, *Science* **244**, 967, note 32 (1989)]. However, accessible porosity in the substrate of the ice stream at our drill site must be filled with either water or ice, because the bed is 700 m below sea level there. This precludes drainage of water into an air-filled porous substrate at subfreezing temperatures.
19. A. J. Gow, *Int. Assoc. Hydrol. Sci. Publ.* **86**, 78 (1970); H. T. Ueda and D. E. Garfield, *ibid.* **86**, 53 (1970).
20. Density adjustment from temperatures in the Byrd profile (*19*) to those in the Upstream B profile (Fig. 2) was made with a bulk thermal expansion coefficient of 1.5×10^{-4} K^{-1}. Densities of ice and water were also corrected for compression under pressure at depth using compressibilities of 1.3×10^{-5} bar^{-1} for ice and 5.1×10^{-5} bar^{-1} for water. A smooth transition from the Upstream B ice densities at depths less than 50 m (*16*) and the Byrd ice densities at greater depth (*19*) is made by linear interpolation between the Upstream B value at 47 m and the Byrd value at 150 m. Because near-surface densification is more rapid at Upstream B than at Byrd (*16, 19*), any error in this procedure is likely to result in a calculated flotation level that is somewhat too deep.
21. Some or all of these effects may be artifacts of the pressure measurement technique—for example, from freeze-in of ice around or into the sensing orifice of the pressure-transducer package. This possibility is suggested in that the second pressure rise began just at the time the transducer operation was switched from readings every 10 min to every 1 hour, which resulted in a consequent reduction in average heat dissipation by the transducer unit. The possibility is, however, opposed by the melting condition at the bed (where the transducer was located), which should preclude freeze-in.
22. R. P. Scherer, *Antarc. J. U.S.*, in press; for a comparison with micropaleontological evidence from under the Ross Ice Shelf see (*23*).
23. R. P. Scherer, D. M. Harwood, S. E. Ishman, P. N. Webb, *Antarc. J. U.S.* **23**, 34 (1988); D. M. Harwood, R. P. Scherer, P. N. Webb, *Mar. Micropaleontol.* **15**, 91 (1989); D. E. Kellogg and T. B. Kellogg, *Micropaleontology* **32**, 74 (1986).
24. L. Drake, in *Till, a Symposium*, R. P. Goldthwaite, Ed. (Ohio State Univ. Press, Columbus, 1971), figure 7, p. 82.
25. R. A. Freeze and J. A. Cherry, *Groundwater* (Prentice-Hall, Englewood Cliffs, NJ, 1979), table 2.2, p. 29.
26. S. T. Rooney, D. D. Blankenship, R. B. Alley, C. R. Bentley, *J. Geophys. Res.* **92**, 8913.
27. B. Kamb *et al.*, *Science* **227**, 469 (1985); B. Kamb and H. Engelhardt, *J. Glaciol.* **33**, 27 (1987); A. Iken and R. A. Bindschadler, *ibid.* **32**, 101 (1986).
28. W. F. Budd *et al.*, *J. Glaciol.* **23**, 157 (1979).
29. A. C. Fowler, *J. Geophys. Res.* **92**, 9111 (1987); A. Iken, *J. Glaciol.* **27**, 407 (1981); L. Lliboutry, *ibid.* 7, 21 (1968); J. Weertman, *ibid.* **5**, 287 (1964).
30. G. S. Boulton, and R. C. A. Hindmarsh, *J. Geophys. Res.* **92**, 9059 (1987); W. H. Matthews and J. R. Mackay, *Trans. R. Soc. Can. Sect. 4* **54**, 27 (1960).
31. This work was supported by the U.S. National Science Foundation under grant DPP-8519083. We thank R. P. Scherer and H. A. Lowenstam for paleontological information and J. Chadwick, M. Wumkes, J. Berkey, H. Aschmann, M. Blume, H. Conway, S. Duncan, T. Svitek, and J. Zachariasen for help in the field work. Contribution No. 4791, Division of Geological and Planetary Sciences, California Institute of Technology.

16 November 1989; accepted 30 January 1990